Combined Finite–Discrete Numerical Modeling of Runout of the Torgiovannetto di Assisi Rockslide in Central Italy

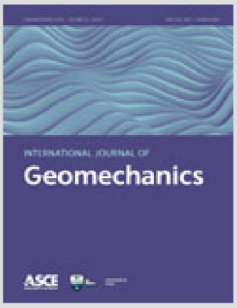

This paper is published on International Journal of Geomechanics, American Society of Civil Engineers (ASCE), Reston (VA), USA (DOI: 10.1061/(ASCE)GM.1943-5622.0000646).

The final publication is avalable at: http://ascelibrary.org/doi/10.1061/%28ASCE%29GM.1943-5622.0000646

Combined Finite-Discrete numerical modeling of runout of the Torgiovannetto di Assisi rockslide in Central Italy

Francesco Antolini *[1], Marco Barla [2], Giovanni Gigli [3], Andrea Giorgetti [4], Emanuele Intrieri [5], Nicola Casagli [6]

[1] Research Assistant, Dept. of Structural, Building and Geotechnical Engineering, Politecnico di Torino, Corso Duca degli Abruzzi 24, 10129 Torino, Italy (corresponding author). E-mail: francesco.antolini@polito.it

[2] Research Associate, Dept. of Structural, Building and Geotechnical Engineering, Politecnico di Torino, Corso Duca degli Abruzzi 24, 10129 Torino, Italy.

[3] Research Associate, Dept. of Earth Sciences, Univ. degli Studi di Firenze, Via La Pira 4, 50121 Firenze, Italy.

[4] Associate Professor, Dept. of Electrical and Information Engineering Guglielmo Marconi, Univ. di Bologna, Viale Risorgimento 2, Bologna, Italy.

[5] Research Assistant, Dept. of Earth Sciences, Univ. degli Studi di Firenze, Via La Pira 4, 50121 Firenze, Italy.

[6] Professor, Dept. of Earth Sciences, Univ. degli Studi di Firenze, Via La Pira 4, 50121 Firenze, Italy.

Abstract

The combined finite-discrete element method (FDEM) is an advanced and relatively new numerical modelling technique that combines the features of the FEM with those of the discrete-element method. It simulates the transition of brittle geo-materials from continua to discontinua through fracture growth, coalescence and propagation. With FDEM it is possible to simulate landslides from triggering to runout and carry out landslides scenario analyses, the results of which can be successively adopted for cost-effective early warning systems. The purpose of this paper is to describe the results of the FDEM simulations of the triggering mechanism and the evolution scenarios of the Torgiovannetto di Assisi rockslide (central Italy), a depleted limestone quarry face where a rock wedge with an approximate volume of 182,000 m^3 lies in limit equilibrium conditions, posing relevant issues in terms of civil protection. The results obtained demonstrate that the FDEM is able to realistically simulate the different phases of such complex slope's failure as well as to estimate both its runout distances and velocity, key features for landslides risk assessment, and management.

Keywords: Numerical modelling; Finite-discrete-element method (FDEM); Rockslide; Triggering; Runout.

Introduction

Today, rock slope stability analysis are routinely performed in order to assess the equilibrium conditions of landslides. A wide range of modelling tools capable to back-analyzing and/or predicting the behaviour of rock slopes are available to engineers and geoscientists. Limit equilibrium analysis represents the most simple and common solution adopted in rock engineering. Major rock slope instabilities, however, involve complex internal deformation and fracturing, bearing little resemblance to the two-dimensional (2D)/three-dimensional (3D) rigid block assumptions adopted in most limit equilibrium analyses (Stead et al. 2006). Furthermore, important limitations of the limit equilibrium method include the limited possibility to take into account progressive failure and deformability of the rock material along with the strength degradation related to the sliding mass deformation. Nowadays, numerical methods offer improved tools to study the complexities related to the geometry, material anisotropy, nonlinear behaviour, in situ stress conditions and coupled processes. Different methods are currently available for rock slope stability analysis. These can be subdivided into the following:

- Continuum methods [e.g., FEM, finite differences method (FDM), boundary elements method (BEM), etc.];
- Discontinuum methods [e.g., distinct-element method (DEM), discontinuous deformation analysis (DDA), particle flow methods (PFM), etc.];
- Hybrid continuum-discontinuum methods [e.g., combined finite-discrete-element method (FDEM), hybrid DEM/BEM methods, other hybrid FEM/DEM methods etc.].

The continuum and the discontinuum numerical methods can be considered as conventional modeling techniques because of their widespread diffusion among the scientific and technical community. The concepts of continuum and discontinuum should not be considered as absolute, but instead they are relative and problem-specific, highly depending on the problem scales. As a consequence, continuum modeling is best suited for the analysis of the intact rock behaviour at the small scale and for the analysis of good and very good quality rock masses [typically with a Geological Strength Index (GSI) $\geq$60] or very jointed rock masses or soil-like material (GSI$\leq$30) at the slope scale. Special joint elements can only allow to model few discontinuities inside the rock mass. Discontinuum modeling is hence more appropriate when the slope evolution is strictly controlled by the relative movements of joint-bounded blocks and the intact rock deformation between them. This is generally more common when the rock mass quality expressed in terms of GSI is between 30 and 60. With the discontinuum, modeling large relative displacements can take place at the contact between each distinct element.

Even though the continuum and the discontinuum methods are also capable of simulating certain aspects of the progressive failure of geomaterials, they often fail to realistically capture and simulate the progressive failure of rock slopes and, in particular, the dynamics of kinematic releases accompanying the distortion, stress concentration, the fracture initiation and subsequent propagation. The need to include the concepts of fracture mechanics has emerged in the last few years as a key issue for rock slope modeling (Stead et al. 2004). The first attempts to address the influence of fracture mechanics on a numerical code date back to the 1980s, when several authors (i.e., Cundall and Strack 1979; Dowding et al. 1983; Lorig et al. 1986; Mustoe 1992; Williams et al. 1985) developed special elements that incorporated fracture to be adopted in the framework of DEM, developed hybrid approaches (i.e. DEM-BEM, FEM-rigid block elements) or started to adopt particle-like formulation of discontinua for the analysis of jointed rock masses. Other attempts to reproduce the fracture processes with numerical methods include, for instance, the work of Saouma and Kleinosky (1984), where the crack initiation and the subsequent crack propagation were simulated in the process of a major chip formation with the finite element code *SICRAP*; the work of Swenson and Ingraffea (1988), through the use of the finite-element code *CRACKER* to model the dynamic propagation of a discrete crack; the work of Wawrzynek and Ingraffea (1989), with the finite element *FRANC2D* software; and the work of Alehossein & Hood (1996), who used both *DIANA* and *NUMA* codes to simulate crack indentation

problems. In the early 1990s a new numerical approach FDEM, which combines both the advantages of FEM and DEM and is capable to model the transition from continua to discontinua, was proposed by Munjiza et al. (1995). In the FDEM each discrete element is modeled through a finite element mesh and the transition from continua to discontinua is modeled through a combination of smeared and discrete crack model. The Munjiza's FDEM method was subsequently implemented in the Y-Code (Munjiza 2004) both for modeling 2D and 3D problems. *ELFEN* is a further example of combined FDEM code. The combined FDEM method makes it possible to reproduce, in a realistic way, the progressive fracture and fragmentation processes and to model the interaction between the distinct elements (i.e., blocks) subsequently generated, modeling thus the runout and the deposition phases of rock landslides (Barla et al. 2011, 2013; Barla and Antolini, 2012; Piovano et al. 2013; Stead and Coggan 2006; Stead et al. 2006).

In this paper, the results of the FDEM simulations of the triggering mechanisms and the runout of the Torgiovannetto di Assisi rockslide (central Italy), a depleted limestone quarry face affected by stability problems, are described and discussed in details. The FDEM models to be adopted in the scenario analysis were previously calibrated through a back analysis of a bench-scale failure that occurred in December 2005. Specific laboratory tests were also carried out to determine the geotechnical parameters that control the fracture propagation in the FDEM models. Moreover, a uniaxial compression test was reproduced by means of FDEM and the results were compared with the experimental ones in order to verify the reliability of the software adopted.

Combined FDEM

The original Y-Code was developed by Munjiza et al. (1995) as a 2D open source software written in C++, capable of modeling continuum and discontinuum behaviour of geomaterials. Despite the great potential of Y-Code, the original version has revealed a number of key limitations when applied to rock mechanics problems which were addressed by the creation of the Y-Geo code (Mahabadi et al. 2010a; 2012). Therefore Y-Geo is actually the version of the original Munjiza's code optimized to model geomechanical problems.

The finite-discrete numerical method combines the principles of continuum mechanics with DEM algorithms to simulate the behaviour of multiple interacting bodies. Each single body of the modeled domain is associated with a deformable finite-element mesh consisting of triangular elements and nodes. In addition to be deformable, each body can fracture and the subsequent particles generated can interact with each other. Two key algorithms of the method (the contact detection and the contact interaction) control the behaviour of the interacting distinct elements. As soon as the discrete bodies are detected in contact, the interaction algorithm calculates the contact forces both between the discrete bodies and along internal discontinuities (i.e., pre-existing and newly created fractures). A penalty function method is used to enforce bodies' impenetrability in the normal direction, thus generating contact forces, which depend on the shape and on the size of the overlap between the contacting elements. Given the cohesive crack model implemented in the FDEM method, specific four-nodes cohesive fracture elements are inserted between the triangular three nodes elements. Therefore the material strain is expected to be localized in the cohesive zone. The bulk material is instead treated as a linear elastic medium using constant-strain triangular elements. Before the cohesive strength is exceeded, a finite stiffness is required by the time-explicit formulation of FDEM to limit deformation of the crack elements. Such an artificial stiffness is represented numerically by the normal, tangential and fracture penalty values, for compressive, shear and tensile loading conditions, respectively. An exhaustive explanation of the penalty function methods for FDEM method can be find in Munjiza and Andrews (2000).

In the tangential direction the discontinuity frictional behaviour is simulated by a Mohr-Coulomb frictional law, resulting in shear interaction forces between each element. A time-marching explicit integration scheme is applied to solve the equations

of motion for the discretised system and to update the nodal coordinates at each simulation time step (i.e., fully dynamic simulations can be performed). A numerical viscous damping (i.e., proportional to velocity) is introduced in the constitutive equation either to account for energy dissipation due to nonlinear material behaviour or to model quasi-static phenomena by means of dynamic relaxation (Munjiza 2004). The nonlinear response of a system is accomplished through fracture and fragmentation (i.e., in essence the process of transition from continua to discontinua). The progressive failure of rock material is simulated in FDEM according to the principles of non-linear elastic fracture mechanics (Dugdale 1960, Barenblatt 1962) assuming a combined single and smeared cohesive crack model, also known as a discrete crack model. The fracture processes are accomplished through specific four-nodes crack elements that are inserted at the interface between each side of the plane stress elastic three-nodes elements. The fracture is allowed only between the elements sides and no adaptive remeshing algorithms are adopted. The development of fracture and fragmentation are therefore sensitive to both element size and element orientation. However, if appropriate element size is used compared to the scale of modeled problem, this influence can be sensibly limited, obtaining satisfactorily results (Munjiza & John 2002, Piovano et al. 2011).

Based on the normal stresses acting on each potential failure surfaces, the four-nodes crack elements inserted between each triangular element of the mesh behave elastically until the strength limit defined by a Mohr-Coulomb failure criterion with a tension cutoff is reached:

$$\begin{aligned} f_s &= f_t && if \quad \sigma_n < f_t \\ f_s &= \sigma_n tan\varphi' + c' && if \quad \sigma_n \geq f_t \end{aligned} \tag{1}$$

where f_s =shear strength, f_t = tensile strength, σ_n = normal stress acting on the potential failure surface; φ' = effective friction angle and c' = effective cohesion of the intact material. Upon overcoming the limit, a new fracture is therefore driven across the interface between adjacent triangular finite elements. Therefore the potential crack paths do not need to be assumed a priori, and arbitrary fracture trajectories can be captured within the constraints imposed by the initial mesh topology.

To specifically account for the loss in kinetic energy during impacts, a new energy dissipation mechanism was added to the original Y-Code (Lisjak & Grasselli 2010, 2011). Such dissipation mechanism, modeled through an elastic-power damping contact constitutive law (An & Tannant 2007), is similar to a normal restitution coefficient expressed in term of ratios of pre- and postimpact kinetic energy or velocity and can be adopted to realistically simulate the energy dissipated in the impact of moving masses.

The aforementioned features make the FDEM appropriate for modeling slope stability problems, the main advantage being the possibility to simulate the transition from continua to discontinua by fracturing and fragmentation processes. This allows for modeling the triggering, initiation, transport and deposition phases of a landslide with a unique tool, overcoming the specific limitations of continuum and discontinuum methods, respectively.

To model a slope stability problem, the FDEM analysis has to be performed in two stages:

1. The first stage is carried out to set the initial in situ stress state conditions, due to the gravitational field. All materials are assumed to behave according to a linear elastic constitutive model in this stage. The total kinetic energy is monitored to assess full equilibrium, and the analysis is interrupted when its value is close to zero.
2. The updated nodal coordinates and velocities are used as inputs for the second stage where fracture propagation along the element edges is allowed, both for mode I (tension) and mode II (shear).

As a validation exercise, Y-Geo was used to simulate a uniaxial compression laboratory test performed on the Maiolica limestone. An intact rock specimen of 50-mm diameter, with a height-to-diameter ratio of 2:1, was modeled by an

unstructured mesh (average element size equal to 0.6 mm) generated with *CUBIT* using a Delaunay triangulation scheme. Each loading platen was modeled as a single discrete triangular element.

The properties of the Maiolica intact rock are listed in Table 1, whereas the numerical properties used in the simulations are shown in Table 2. The depicted Young's modulus was experimentally determined by adopting the measured external axial deformation and is sensibly lower to that given in the literature (i.e., 10.8 versus 71.4 GPa) which was used in the subsequent simulations at the site scale. A Mohr-Coulomb failure criterion with tension cutoff was assumed for the rock material and a friction coefficient of 0.09 (equivalent to 5.0°) is assumed between the rock sample and the loading platens.

Table 1 – Material Properties Adopted for FDEM Simulation of Uniaxial Compression Test

Material property	**Maiolica limestone**	**Loading platens**
Elastic modulus (E) (GPa)	10.8	200.0
Poisson's Ratio (ν)	0.26	0.29
Density (kg/m^3)	2640	8000
Friction angle (φ') (°)	41.0	5.0 [a]
Cohesion (c') (MPa)	16.9	-
Tensile strength (σ_t) (MPa)	5.76	-
Fracture Energy mode I (G_f) (J/m^2)	25.0	-
Fracture Energy mode II (G_s) (J/m^2)	50.0	-

[a] Friction angle assigned to the contact between the loading platens and the rock sample

Table 2 – Numerical Parameters Adopted For FDEM Simulation of Uniaxial Compression Test

Numerical parameter	**Maiolica limestone**	**Loading platens**
Viscous damping (kg/ms)	7.5E+06	2.9E+08
Normal contact Penalty (GPa·m)	108.0	2000.0
Tangential contact Penalty (GPa/m)	10.8	200.0
Fracture penalty (GPa)	1.08	-

To simulate the uniaxial compression test, a constant vertical velocity equal to 0.35 mm/s was applied to the loading platens. In the real laboratory test a quasi-static displacement rate was applied (i.e., $8.3 \cdot 10^{-4}$ mm/s). However, the size of time step needed to satisfy the stability condition of the explicit time integration using such loading velocity scheme would have resulted in an unacceptably long computational time. Parametric analyses on the application of different loading velocities with FDEM simulations have demonstrated that the quasi-static condition can be obtained by using a relatively high displacement rate, such as 0.5 mm/s (Mahabadi et al. 2010b).

In Figure 1 the stress-strain curves obtained from the numerical modeling are compared to that measured in the laboratory along with the fracture pattern evolution retrieved in the numerical simulation. The numerical results are in good agreement with the experimental ones thus confirming the capability of FDEM to realistically and quantitatively model the failure of a homogeneous rock specimen under uniaxial stress conditions. The brittle behavior of the limestone material is well captured: tensile and shear fractures start to form at the center of the rock sample, developing, in a short time, to a major shear failure plane inclined approximately at 65-70° from the horizontal axis. For greater axial strain, further tensile cracks continue to propagate mainly in the axial direction [i.e., parallel to the direction of the principal stress (σ_1)], leading to the complete failure of the specimen.

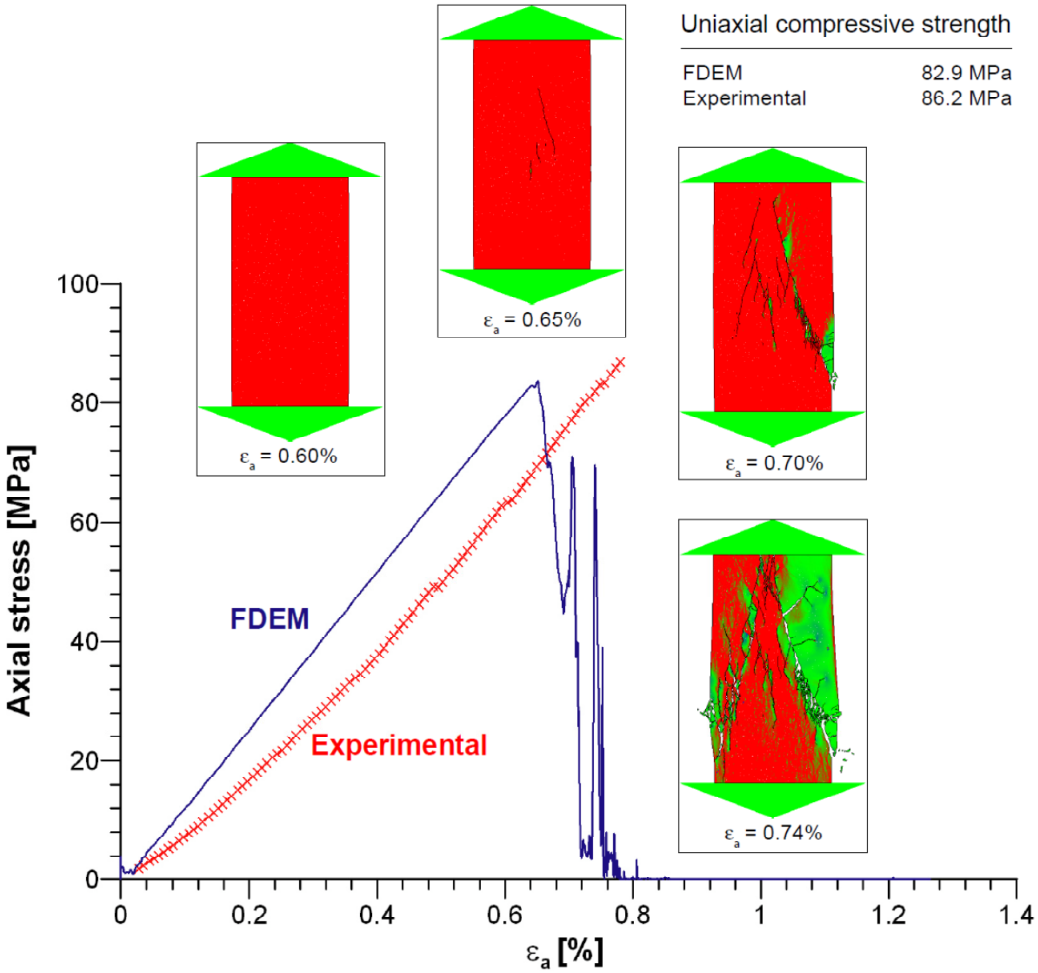

Figure 1 – Comparison between experimental results and FDEM numerical simulation for the uniaxial compression test on Maiolica limestone and fracture patterns at different axial strains

Torgiovannetto di Assisi Rockslide

The Torgiovannetto rockslide is located in central Italy (Figure 2) and represents a well-known landslide in a depleted limestone quarry site that is widely described in literature (Brocca et al. 2012; Gigli et al. 2007; Graziani et al. 2009; 2010; Intrieri et al. 2012; Salciarini et al. 2009). The instability issues in the Torgiovannetto quarry are mainly a consequence of the former mining activities, along with the structural setting and the sedimentary characteristics of the quarried limestones belonging to the Maiolica Formation. Maiolica consists of regularly thin-stratified (5-100 cm) micritic limestones interbedded with centimeters-thick (1-30 cm) greenish-grey clayey marls characterized by a dip between 24° and 31° and a regular dip in the north direction, concordant with the orientation of the main quarry face (Figure 3). The most diffuse instability mechanism, as shown in Figure 4, is therefore the planar sliding along the bedding planes (BG) promoted by the presence of the marly-clay interlayer and delimited by three nearly orthogonal, subvertical and very persistent joint sets (K1, K3a-b and K2).

The main rock wedge instability in the Torgiovannetto quarry was first recognized in 2003 and is still in existence, posing relevant issues in terms of civil protection, because two important roads are located downslope. The failure was recognized by the progressive opening (up to 2 m) of a nearly continuous perimetral tension crack and the slipping of the rock mass along a

persistent marly-clayey bedding joint (Figure 3). The rock wedge is still progressively sliding along the weak bedding plane, with acceleration and deceleration phases substantially governed by the seasonal rainfall regime. The volume involved in the sliding was estimated to be 182,000 m^3.

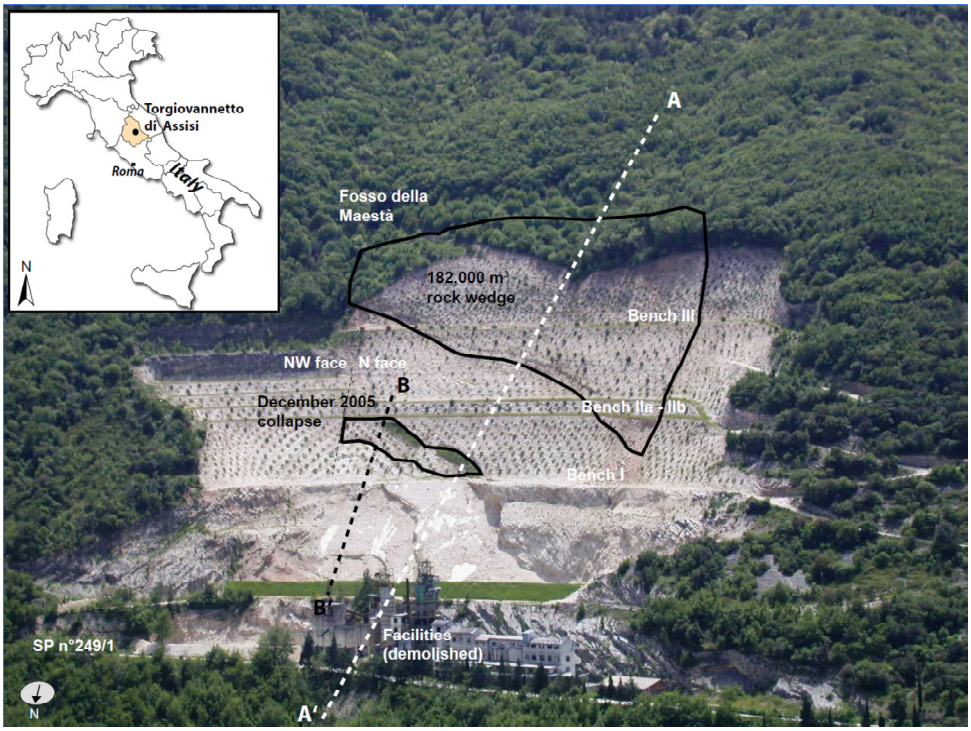

Figure 2 – Bird's eye view of the Torgiovannetto quarry in 2004; the 182,000-m3 unstable rock wedge is shown along with the cross sections adopted for the FDEM models (A-A' and B-B') and the wedge collapsed in December 2005 (image by Giovanni Gigli)

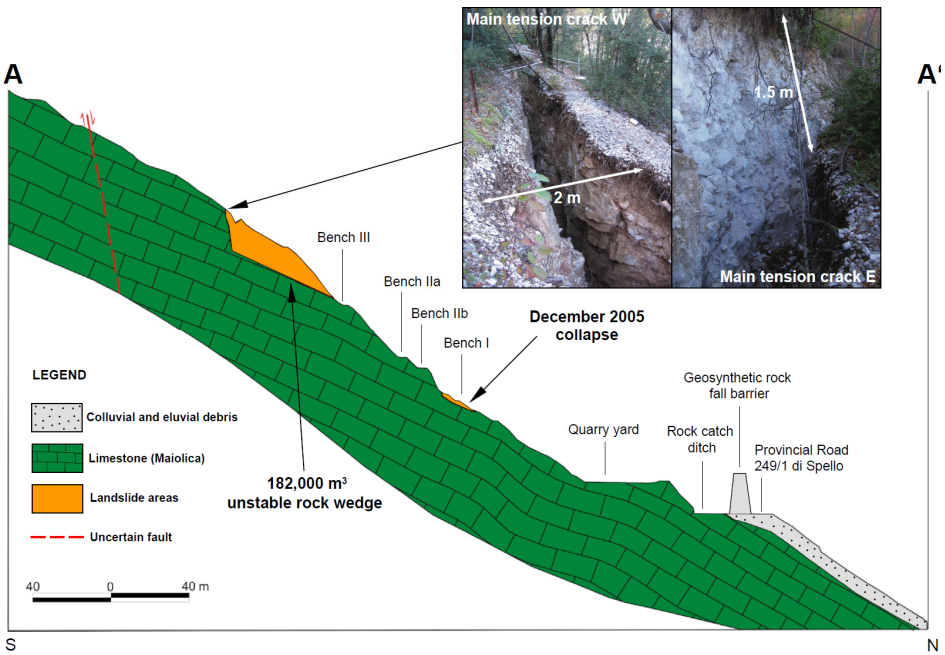

Figure 3 - Geologic cross section of the Torgiovannetto quarry (A-A' in Figure 2) with indication of the active landslide (adapted from Balducci et al. 2011; images by Francesco Antolini)

A bench-scale collapse, with similar geometry and an approximate volume of some thousands of cubic meters, occurred in December 2005 after a period of prolonged rainfall, confirming the instability mechanism affecting the quarry face and providing further insights for the understanding of the behaviour of the slope (Figure 4).

Since 2003, the displacement pattern of the Torgiovannetto quarry was discontinuously monitored by means of topographic measures, wire and bar extensometers installed across the main open fractures (Graziani et al. 2009; Intrieri et al. 2012) and Ground-Based Interferometric Synthetic Aperture Radar (GBInSAR) surveys (Canuti et al. 2006; Atzeni et al. 2015; Barla and Antolini 2015).

During 2013, a new GBInSAR survey was carried out, and a new wireless sensor network (WSN) consisting of wire and bar extensometers, tiltmeters, soil moisture probes and a weather station was installed on the Torgiovannetto landslide. It should be pointed out that remote sensing techniques are more and more often used for landslide hazard assessment and analysis. Although remote sensing provides very high spatial resolution and coverage, it requires accurate installation and calibration procedures. From a different perspective WSNs can quickly respond to rapid changes of relevant physical parameters and send them to a remote centre for further elaboration and alerting (Buratti et al. 2005; Hart & Martinez 2006; Verdone et al. 2010; Giorgetti et al. 2011).

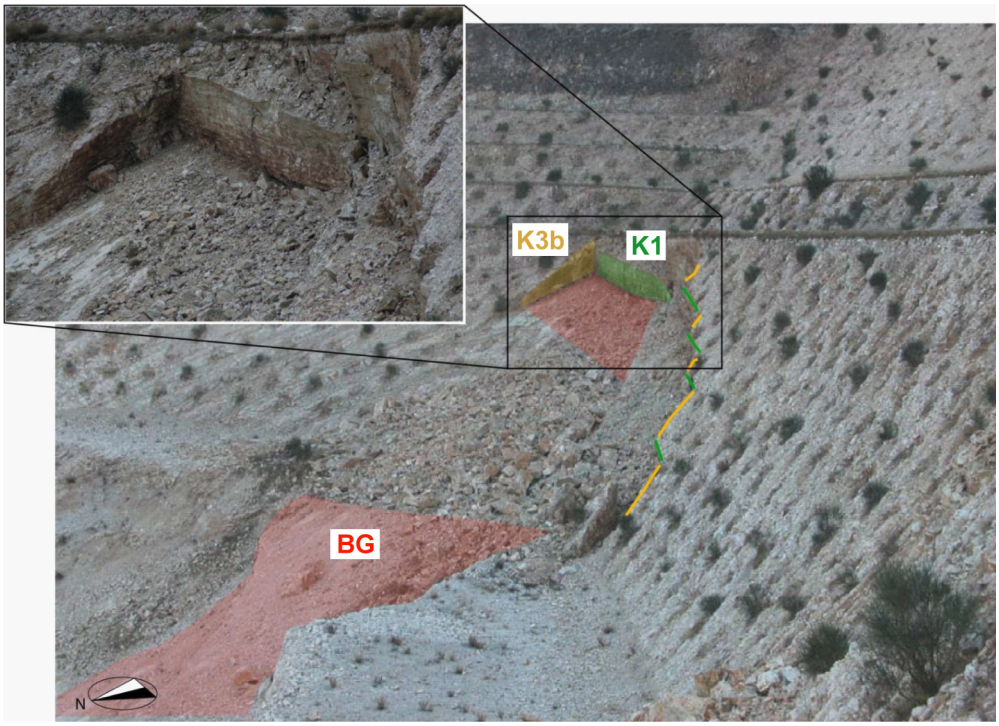

Figure 4 – Close view of the December 2005 bench scale failure highlighting the main discontinuity sets of the rock mass (BG=bedding planes, K1 – K3b=subvertical joint sets)(images by Francesco Antolini and Giovanni Gigli)

The monitoring system allowed confirmation that the displacement pattern of the quarry face is strictly influenced by the seasonal rainfall regime. During wet periods (winter and spring) the crack openings underwent evident long-term acceleration, whereas on dry periods (i.e., summer), the rate of displacement noticeably decreased, tending to zero [Figure 5(a)]. Moreover the GBInSAR survey carried out in 2013 revealed short-term acceleration of the movements in the lower portion of the 182,000-m^3 rock wedge, following intense rainfall events [Figure 5(b) – 5(c)]. Results of limit equilibrium as well as finite

elements simulations with hydro mechanical coupling for the Torgiovannetto landslide have also confirmed aforementioned findings (Graziani et al. 2010).

With the aim of gaining an improved understanding on the mechanical behaviour of the intact Maiolica limestone, a set of standard laboratory tests, including uniaxial, triaxial and indirect tensile strength tests were carried out. The obtained results, along with data available from literature (Graziani et al. 2009, 2010) allowed for the complete characterization of the intact rock, the discontinuities and the rock mass by the estimation of a representative GSI of 40.

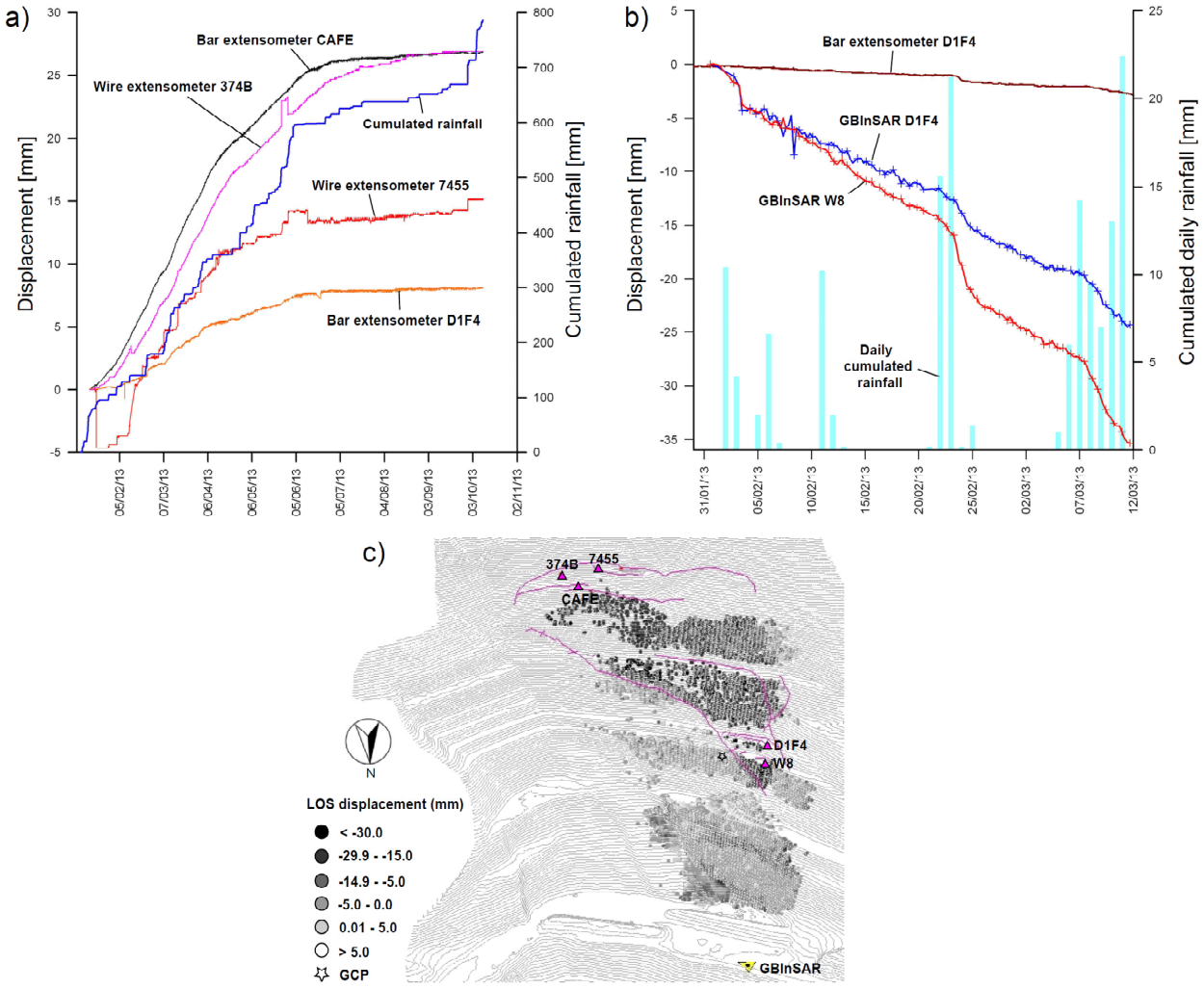

Figure 5 – Monitoring data: (a) fractures opening measured from January to October 2013 by WSN extensometers versus cumulated rainfalls; (b) time series of GBInSAR points located on the lower portion of the unstable wedge versus cumulated daily rainfall; (c) GBInSAR cumulated line-of-sight (LOS) displacement maps with position of the measuring points

Regarding the interbed marly-clayey filling material on the sliding plane of the 182,000-m^3 rock wedge, data available from literature (Graziani et al. 2009, 2010) indicates an effective friction angle equal to 21.3° and an effective cohesion of 21 kPa at peak, with significant variations in the residual friction angle (10° - 17°).

For the combined FDEM modeling, all of the required material and discontinuity properties can be obtained through standard laboratory tests, aside from the fracture energy release rate (Gf). To experimentally determine the value of the fracture energy release rate for mode I cracks (i.e., cracks developed in tension), three prismatic rock samples (T1, T2 and T3)

of Maiolica limestone were tested by means of a three-point bend test on single edge notched beam (SENB) (Malvar & Warren, 1988). Figure 6 shows the arrangement of a SENB and a theoretical force-displacement curve, which represents the direct result of the test. Given the value of U_0 (the area under the force-displacement curve), it is possible to obtain the value of the fracture energy for cracks developed in tension by:

$$G_{fI} = \frac{U_0 + (m_1 + m_2)g\delta_0}{B(W - a_0)} \quad (2)$$

where m_1 and m_2 = mass of the sample which lies between the rollers and mass of the additional supports; g = gravity; δ_0 = maximum inflection of the load point; B = sample height; W = sample width; and a_0 = initial notch length. The load-point displacement was measured by means of two inductive transducers placed along the front and rear faces at the center of the sample (Figure 6). To obtain the final fracture energy release rate, the two values calculated for each U_0 value were averaged. The results of the test denotes a high brittleness of the Maiolica limestone: once the fracture starts to enucleate at the apex of the notch, it immediately propagates, reaching the upper face of the sample with an almost linear path. The fracture energy release rate values (G_{fj}) obtained for each sample tested are between 20.5 and 29.2 J/m² with a mean value equal to 24.1 J/m².

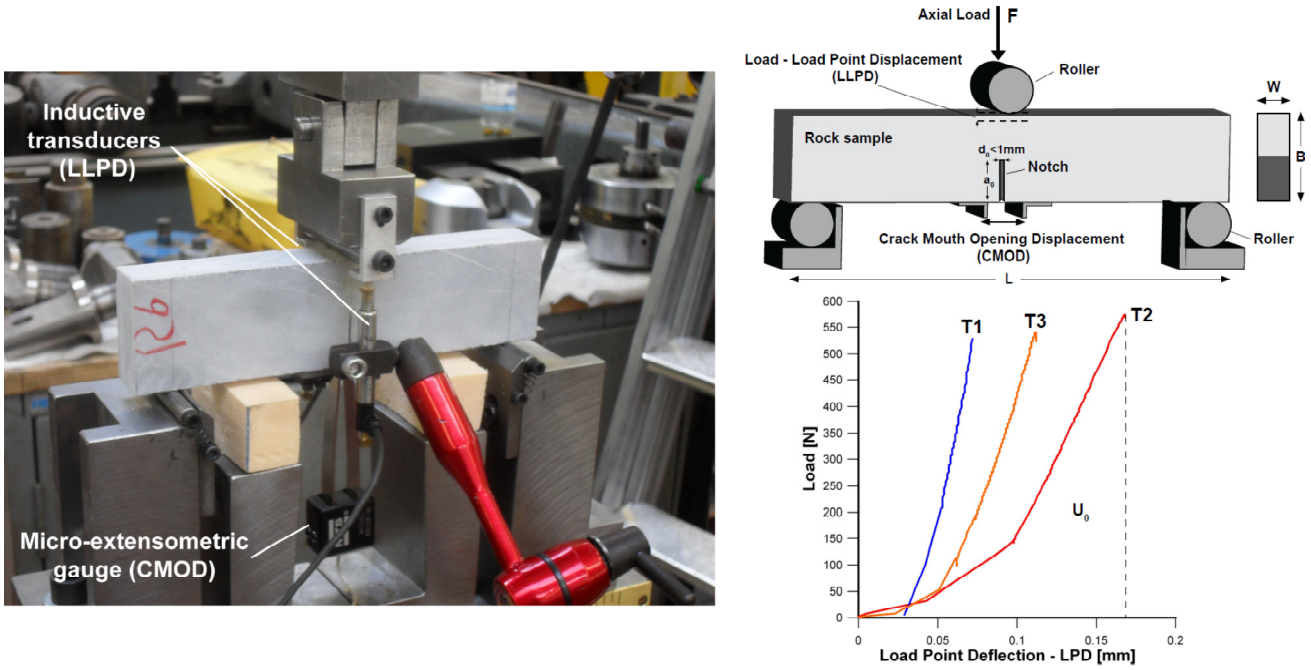

Figure 6 – SENB tests experimental setup and load-load point displacement (LLPD) curves obtained for the three Maiolica samples tested (T1, T2, T3)

Rock Slope Stability Analysis by FDEM

To study the triggering conditions and to simulate the collapse of the 182,000-m³ rock wedge the FDEM was adopted. It is clear that triggering conditions could have been investigated with other well-known methods, such as the limit equilibrium or the continuum or discontinuum numerical methods. This has been done by other Authors (Graziani et al. 2010). A detailed comparative analysis was considered to be outside the scope of this paper. A validation of the mechanical parameters along

with a calibration of the numerical parameters required in the FDEM was carried out by back-analyzing the bench scale failure occurred in December 2005. Therefore, the main purpose of the back-analysis was to reproduce the collapse, fragmentation, and deposition of the collapsed mass and compare it to the real runout data available.

Back Analysis of the December 2005 Instability

Two different modeling approaches were adopted to represent the rock mass in the back analysis process: equivalent continuum and discontinuum. Consequently, two models were built (Back-Analyses 1 and 2), and their cross-sections are shown in Figure 7. The mesh was generated using a 3-noded triangulation scheme with an average element size of 0.28 m for the sliding block and an average element size of 2 m for the rest of the model. The sliding surface, corresponding to a bedding plane with marly-clayey filling, and the tension crack were included in the model as pre-existing discontinuities.

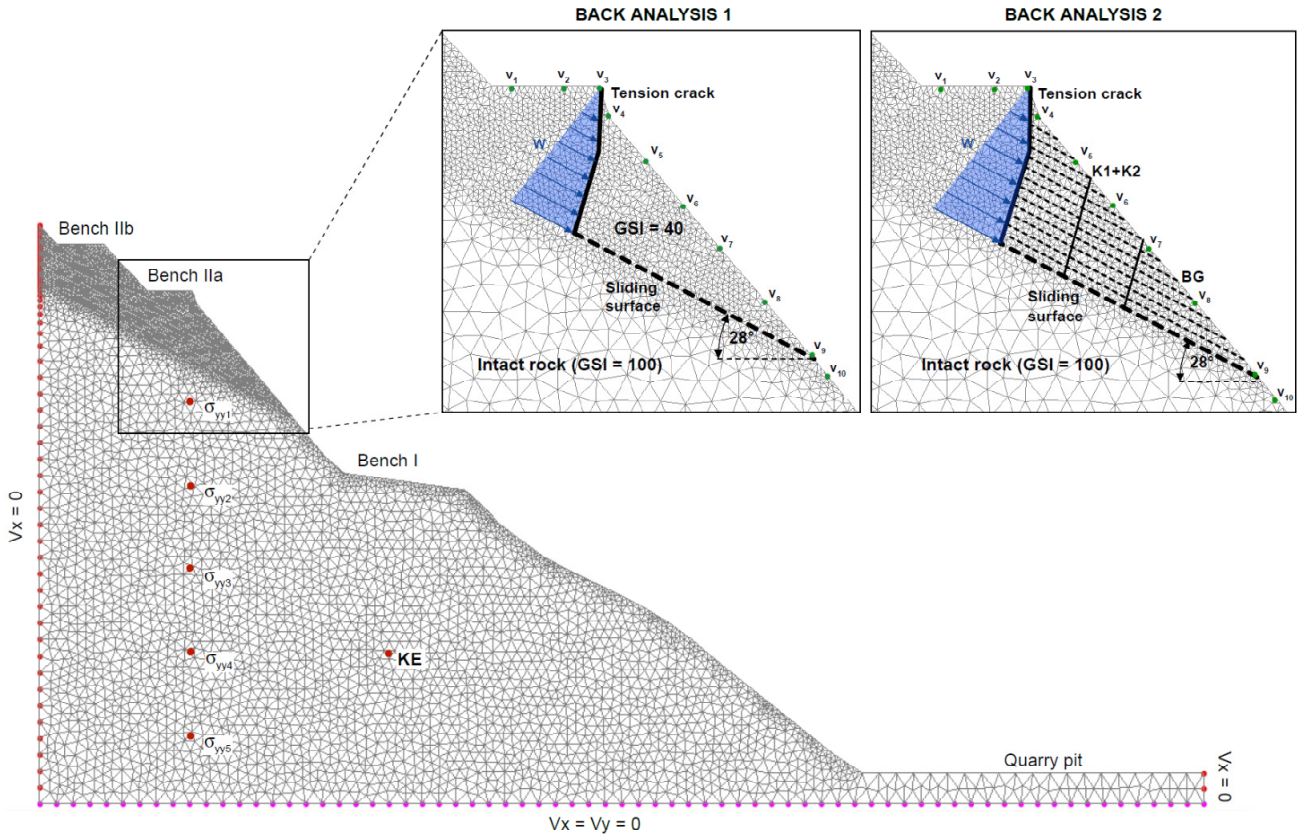

Figure 7 – Mesh and boundary conditions for the two back-analyses of the December 2005 collapse

Plane strain conditions were assumed.

The numerical simulation was performed in two stages:

1. application of the initial in situ stress condition (gravity turn-on), and
2. application of the water pressure in the tension crack and simulation of the slope instability (fracture turn-on).

The December 2005 failure was triggered by the saturation of the sub vertical tension cracks as well as a progressive increase of the pore pressure inside the marly-clayey level, which acted as the sliding plane. For the sake of simplicity, the back analyses were carried out assuming only a complete saturation of the tension crack while discarding the increase in the pore pressure along the sliding plane. The pressure distribution in the tension crack was assumed as hydrostatic. Because the

sliding of the rock wedge causes a progressive opening of the tension crack, the initial pressure distribution was progressively decreased to zero by a linear dissipation function, calibrated in a set of specific analyses.

A normal restitution coefficient was introduced to take into account the inelastic response of the materials and the energy dissipated by the impacts between the different discrete elements. The normal rebound coefficient (R_n) of the slope (i.e., the ratio of the incoming vs. the outgoing velocity of the discrete element) was set to 0.5, considering its surface as mainly composed by clean hard limestone bedrock with thin soil or debris.

In Back Analysis 1, the rock mass was modeled with equivalent continuum parameters and the discontinuities were not inserted explicitly in the mesh. In Back Analysis 2, the discontinuities (bedding planes and K1+K2 joint sets) were included, with their specific mechanical parameters, and intact rock parameters are given to the blocks generated by the discontinuity network. To limit the total number of elements, discontinuities were introduced only in the wedge region. Based on the geotechnical characterization described earlier, the rock mass and the discontinuity properties are given in Table 3, whereas Table 4 shows the numerical properties adopted in the numerical analyses. The main characteristics of the joints and the bedding planes are given in Table 5.

Figure 8 shows the results of the two back analyses. In the case of Back Analysis 1, when triggered by the water pressure in the tension crack, the block starts to move along the basal sliding plane and progressively fractures as a results of the low tensile strength of the material. At first, tensile fractures develop orthogonally to the sliding surface, along a narrow region of the block, while the lower portion of the wedge continues to slide nearly intact along the weak basal plane. Subsequently the upper wedge portion progressively slackens at the base, fractures along the bedding planes and topples on the lower one. Most of the fragmented material deposits on Bench I, forming a talus with an angle approximately equal to the inclination of the sliding plane (28°). Only few blocks overcome Bench I, roll along the quarry face, and reach the quarry pit, travelling not more than 10 m from the slope's toe.

Table 3 – Material and Discontinuity Properties Adopted for the FDEM Analyses of Rockslide

Material and discontinuity properties	**Intact Rock**	**Rock mass (GSI=40)**	**Sliding plane**	**Tension crack**	**BG + K1 + K2**
Elastic modulus E (GPa)	71.4	11.4	-	-	-
Poisson's Ratio ν	0.26	0.26	-	-	-
Density ρ (kg/m^3)	2640	2640	-	-	-
Friction angle φ' (°)	32.0	29.5	21.3	49.7	35.0
Cohesion c' (MPa)	3.03	2.43	0.021	0.0392	0.0
Tensile strength σ_t (MPa)	5.76	0.07	-	-	-
Fracture Energy mode I G_f (J/m^2)	25.0	25.0	-	-	-
Fracture Energy mode II G_s (J/m^2)	50.0	50.0	-	-	-

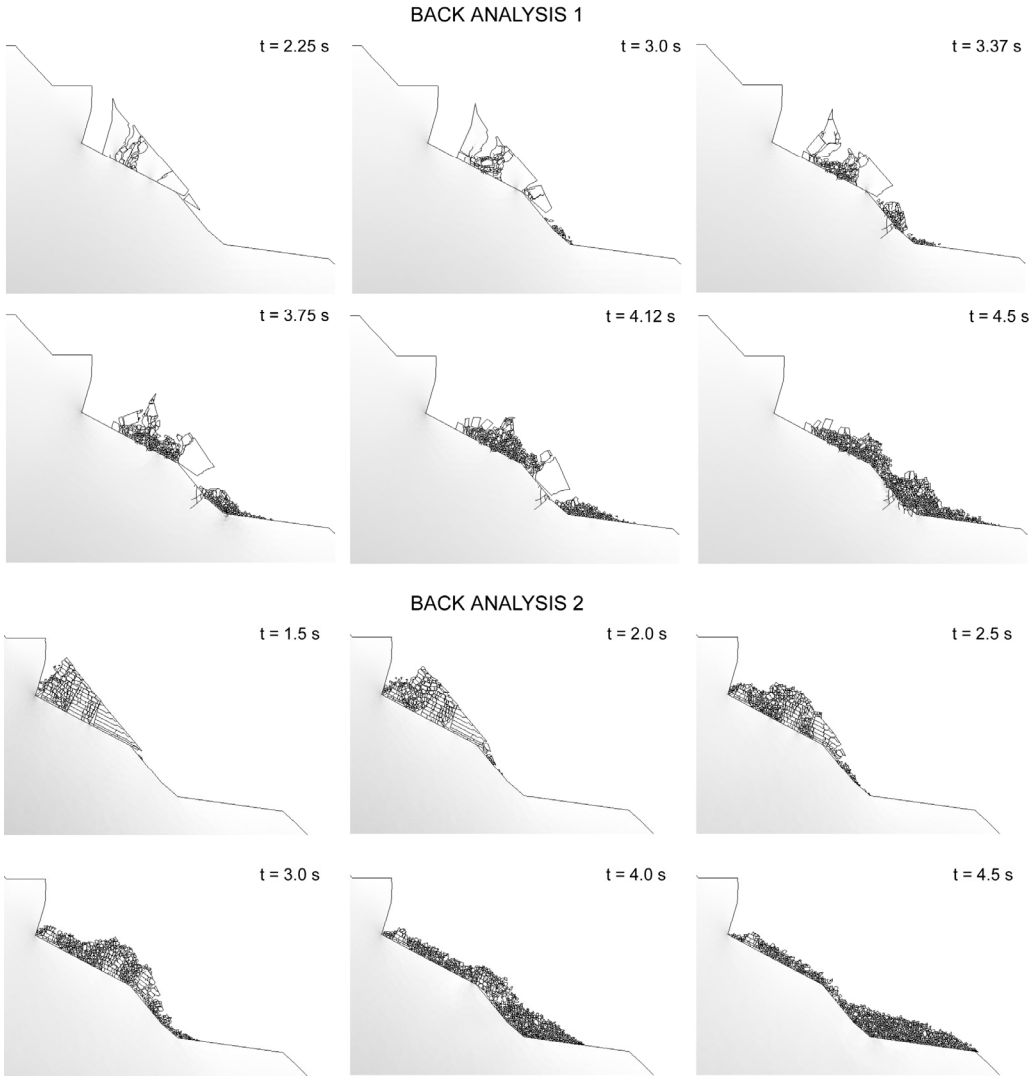

Figure 8 – Results of the Back-Analyses 1 and 2: close view of the collapsed rock wedge

Table 4 – Numerical Parameters Adopted for the FDEM Analyses of Rockslide

Numerical parameter	Back-Analysis 1	Back-Analysis 2	Main wedge analysis	
			Wedge area	External area
Viscous damping (kg/ms)	2.06E+06	4.0E+06	8.3E+06	1.65E+07
Normal contact Penalty (GPa·m)	11.4	43.5	11.4	11.4
Tangential contact Penalty (GPa/m)	1.14	4.35	1.14	1.14
Fracture penalty (GPa)	11.4	43.5	11.4	11.4

Table 5 – Main Characteristics of Joint Sets Adopted in FDEM Model

Joint set	Dip direction (°)	Dip (°)	Persistence (%)	Spacing (m)
BG	005	28	100	0.40
K1 + K2	230	80	100	5-10

In the case of Back Analysis 2, the rapid fracture development leads to a diffuse disarticulation of the rock mass and the generation of toppling-like phenomena of the upper portion of the rock wedge. It is interesting to note that due to a friction angle (35°) of the bedding planes higher than the basal surface (21.3°), sliding along the bedding planes occurs only during the advanced phases of the wedge mobilization.

The runout of the material in the two cases was compared to a detailed digital elevation model of the zone affected by the collapse, obtained by means of a laser scanner survey. As shown in Figure 9, the results of the FDEM simulations are in close agreement with the real runout and deposition of the failed rock mass in both cases, despite a slightly larger volume deposited on the quarry pit in Back-Analysis 2.

Based on the results above, both the equivalent continuum (Back-Analysis 1) and the discontinuum (Back-Analysis 2) approaches were able to realistically reproduce the fracturing and the runout of the collapsed mass. The two back-analyses of the bench collapse allowed the authors to validate the mechanical parameters of the rock mass and the discontinuities, calibrate the numerical parameters required in the FDEM analyses, and provide useful indications to be adopted for the main rock wedge instability simulation. The equivalent continuum approach was chosen for this purpose to simplify mesh generation. Despite the similar geometry of the rock wedges, the two modeled phenomena differ dramatically for the scale of the problem (some thousands of cubic meters versus 182,000 m^3).

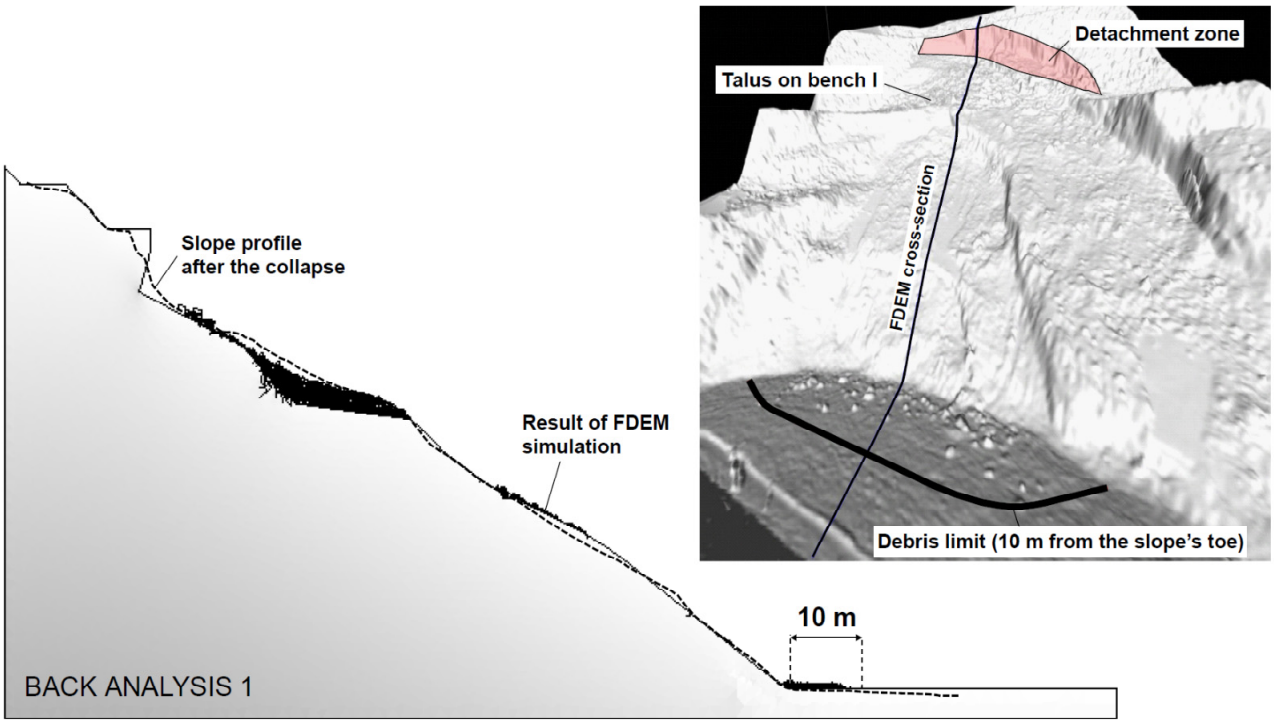

Figure 9 – Comparison between results of the two FDEM simulations and the digital elevation model of the area affected by the December 2005 collapse

Triggering conditions for the main rock wedge

As described previously, the main instability scenario for the Torgiovannetto experimental site is represented by the 182,000-m^3 rock wedge which lies in limit equilibrium conditions. This is studied along the cross section shown in Figure 2. A first set of analyses was run with the scope of evaluating the mechanism that would lead to its catastrophic collapse. Two methods

were adopted to simulate the triggering mechanism: increasing the water height in the tension crack (the same approach adopted for the back analysis) and reducing the shear strength on the basal sliding plane to reproduce the effect of the increasing pore pressures. The mesh adopted for the FDEM models has an average size equal to 1 m in the wedge region and 2 m outside that area. Similar to the back-analysis models, the sliding surface, represented by a persistent bedding plane with the marly-clayey filling, and the tension crack were explicitly included in the model as pre-existing discontinuities. The geometry and the boundary conditions are shown in Figure 10, whereas the mechanical properties and the numerical parameters adopted are listed in Table 3 and in Table 4 respectively. A large-scale undulation along the main sliding plane was already known in literature (Graziani et al., 2010) and was confirmed by the measured variations of the dip direction and the inclination of the bedding planes. For this reason, the basal sliding plane was reproduced with a large-scale roughness profile characterized by an undulation length λ = 5 m and an undulation angle α = 5.25°.

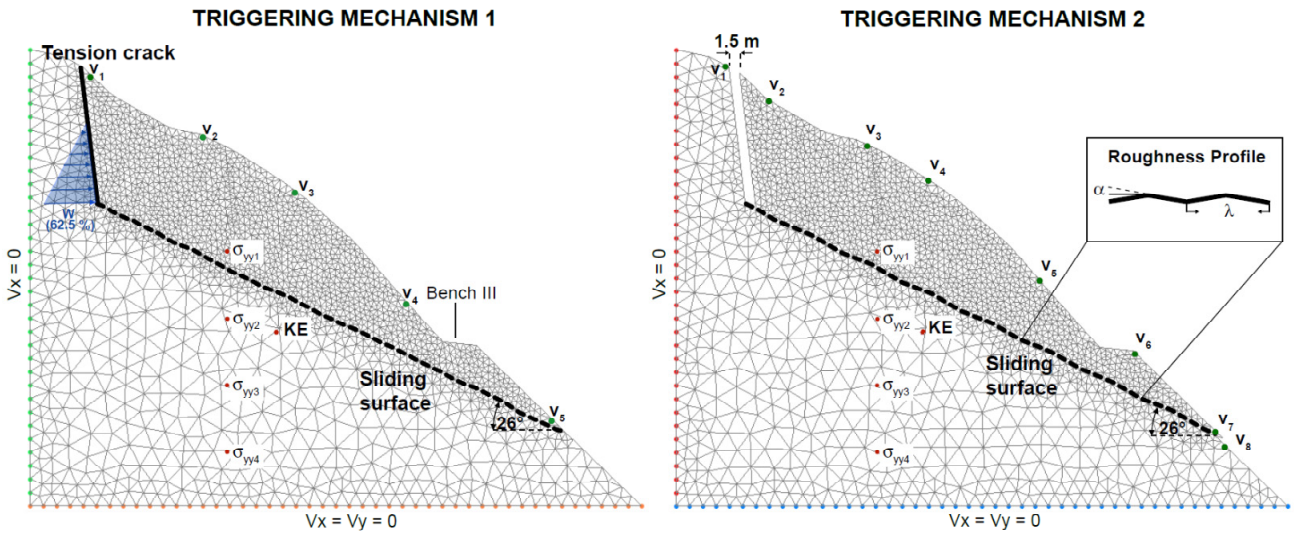

Figure 10 – Geometry, mesh and boundary conditions for the models adopted to study the two triggering mechanisms of the main rock wedge

For the first triggering mechanism, the progressive saturation of the joints induced by prolonged rainfalls was simulated by applying a water pressure in the tension crack. Eight different water heights in the tension crack, equivalent to saturations varying from 25.0 % to 87.5 % of the total depth of the open fracture (20.8 m), were tested. A summary of the simulations performed, along with the resulting stability conditions obtained for the rock wedge is shown in Table 6. The results showed that, for a saturation of the tension crack higher than 54.5% (corresponding to a water head higher than 11.2 m), the wedge becomes unstable and starts collapsing. At first, as the water height in the tension crack increases and reaches 11.7 m (saturation = 56.0%), only the lower portion of the rock wedge becomes unstable. With higher water pressures, the instability progressively extends upslope, leading to the collapse of the whole rock wedge.

To study the second triggering mechanism, for simplicity, the decrease of shear strength on the basal sliding plane resulting from progressive saturation was simulated by modifying the undulation of the plane (i.e., affecting its shear strength). In this case, the geometry of the model was built by including the actual mean opening of the tension crack (1.5 m) and the actual sliding distance covered by the wedge (Figure 10). The surface morphology of the sliding plane was modeled considering a fixed undulation length (λ) equal to 5 m, whereas the undulation angle (α) was progressively decreased to simulate the variation of strength. No water pressure along the tension crack was inserted. A total of 10 simulations were performed and

the results in terms of stability conditions for the rock wedge are shown in Table 7. Instability occurs for undulation angles slightly lower than 5.25°.

The analysis of velocity of the history points located on the slope surface shows for both triggering mechanisms that the attainment of instability conditions is marked by a progressive acceleration of the velocity of the rock wedge (Figure 11), whereas for stable conditions, the velocity progressively reduces to zero. The attainment of instability is also marked by the appearance of an extensive fracturing in the model. The data in Figure 11 are of paramount importance as they were used to define velocity thresholds to be used for the Torgiovannetto landslide's early warning system (Barla & Antolini, 2015).

Table 6 – Results of FDEM Triggering Simulations with Variable Saturation of Tension Crack

Tension crack saturation (%)	**Water height in the tension crack (m)**	**Result**
25.0	5.2	Stable
50.0	10.4	Stable
53.0	11.0	Stable
54.5	11.2	Stable
56.0	11.7	Unstable
62.5	13.2	Unstable
75.0	15.6	Unstable
87.5	18.2	Unstable

Table 7 – Results of FDEM Triggering Simulations with Variable Undulation Angles (α) of Sliding Plane

α (°)	**λ (m)**	**Result**
1.00	5.0	Unstable
2.00	5.0	Unstable
3.00	5.0	Unstable
4.00	5.0	Unstable
4.50	5.0	Unstable
4.75	5.0	Unstable
5.00	5.0	Unstable
5.25	5.0	Stable
5.50	5.0	Stable
6.00	5.0	Stable

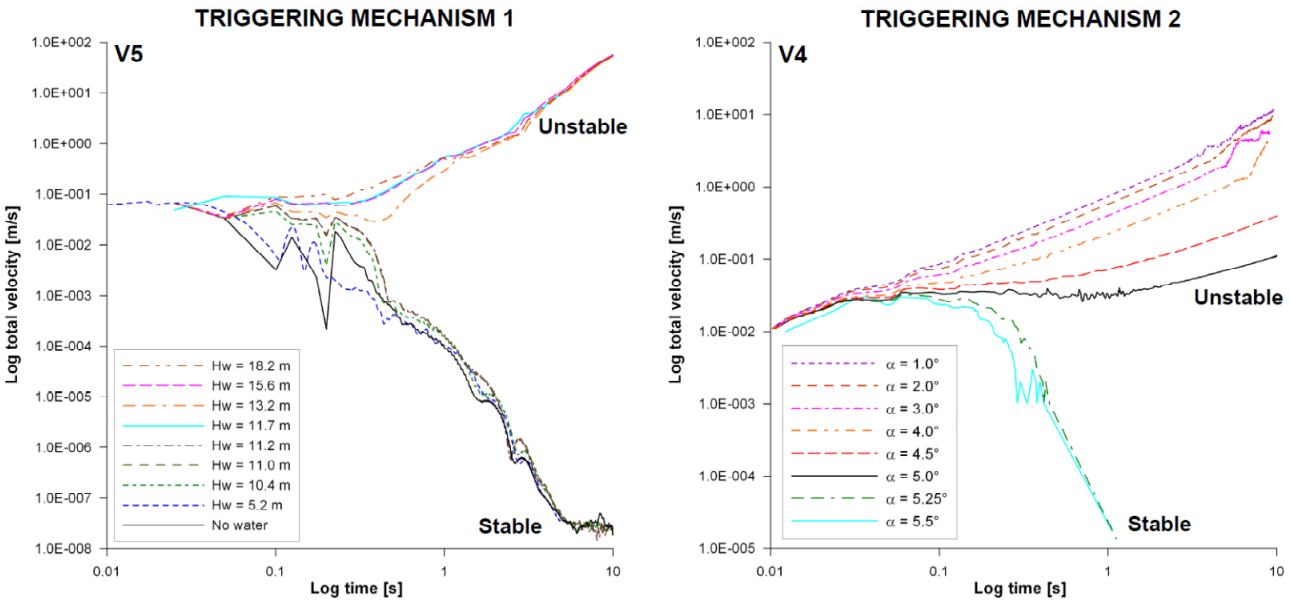

Figure 11 – Bilogarithmic plot of the total velocity computed for the two triggering mechanisms on two selected points (V4 and V5) the positions of which are shown in Figure 9

Runout of Main Rock Wedge

The final step of the FDEM modeling of the Torgiovannetto rockslide was the simulation of the collapse of the rock wedge and its runout. The size of the FDEM model adopted was 345 m wide and 202 m high. The geometry, the mesh, the boundary conditions are shown in Figure 12. Similar to the previous models, the average element size was equal to 1 m in the wedge region whereas was increased to 2 m outside that area. The sliding surface with the roughness profile characterized by λ = 5 m and α = 5.25°, along with the tension crack were explicitly included in the model as pre-existing discontinuities. Mechanical and numerical parameters adopted are given respectively in Table 3 and in Table 4. The normal rebound coefficient (R_n) of the slope was set to 0.5. Again the analysis was run in two stages: the in situ stress state was reproduced in a preliminary stage and fracture was allowed in the subsequent one. The collapse was triggered by applying the water pressure corresponding to 56% of saturation in the tension crack as shown by previous analysis.

The results of the simulation are shown in Figure 13. Following the application of the water pressure in the tension crack, the rock wedge starts to slide along the weak basal bedding plane. The presence of the large scale roughness causes stress concentrations close to the rock asperities after a slight movement of the unstable mass and consequently the generation of tension fractures on the wedge. Progressively, the cracks extend towards the surface causing the separation of the wedge into distinct and independent sectors. This is in good agreement with both what was observed in the field, because the rock wedge is actually crossed out by numerous tension cracks, and the results of the GBInSAR monitoring, which confirmed the presence of different independent kinematic sectors [Figure 5(c)]. The further evolution of the instability showed homogeneous fractures coalescence resulting in a rapid fragmentation of the rock wedge. The collapsed material arrested on the quarry pit forming a talus at the base of the slope, with a repose angle approximately equal to 27°. Only few blocks were able to reach the rock catch ditch area. This short runout is mainly related to the early onset of fracturing and the subsequent extensive fragmentation of the rock mass. Failed rock blocks observed on site were rarely larger than 1 m^3. The extensive fracturing processes, along with contact and friction between the discrete elements, are able to dissipate a high amount of kinetic energy, thus limiting the runout of the failed mass.

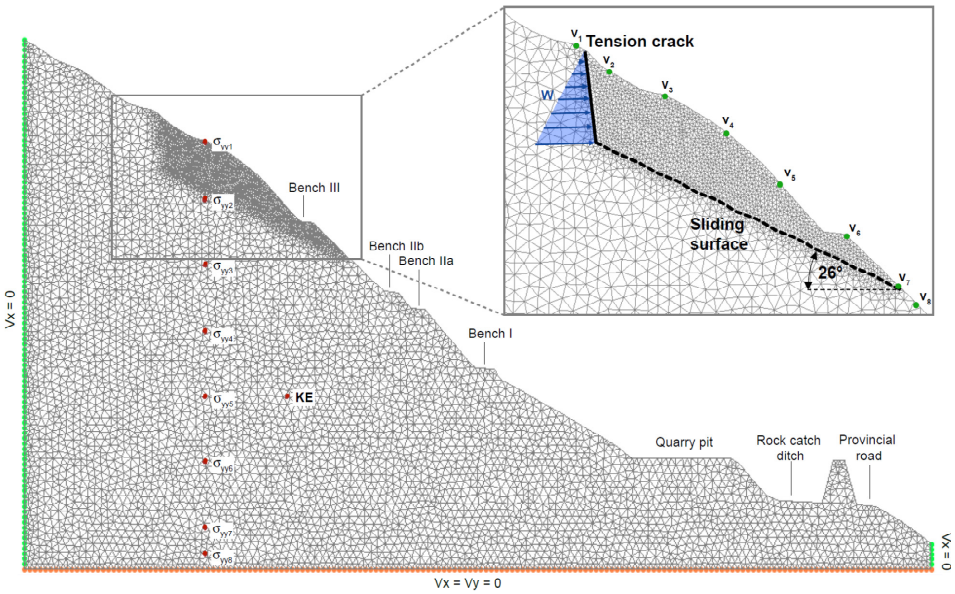

Figure 12 - Geometry, mesh and boundary conditions of the main rock wedge runout FDEM model

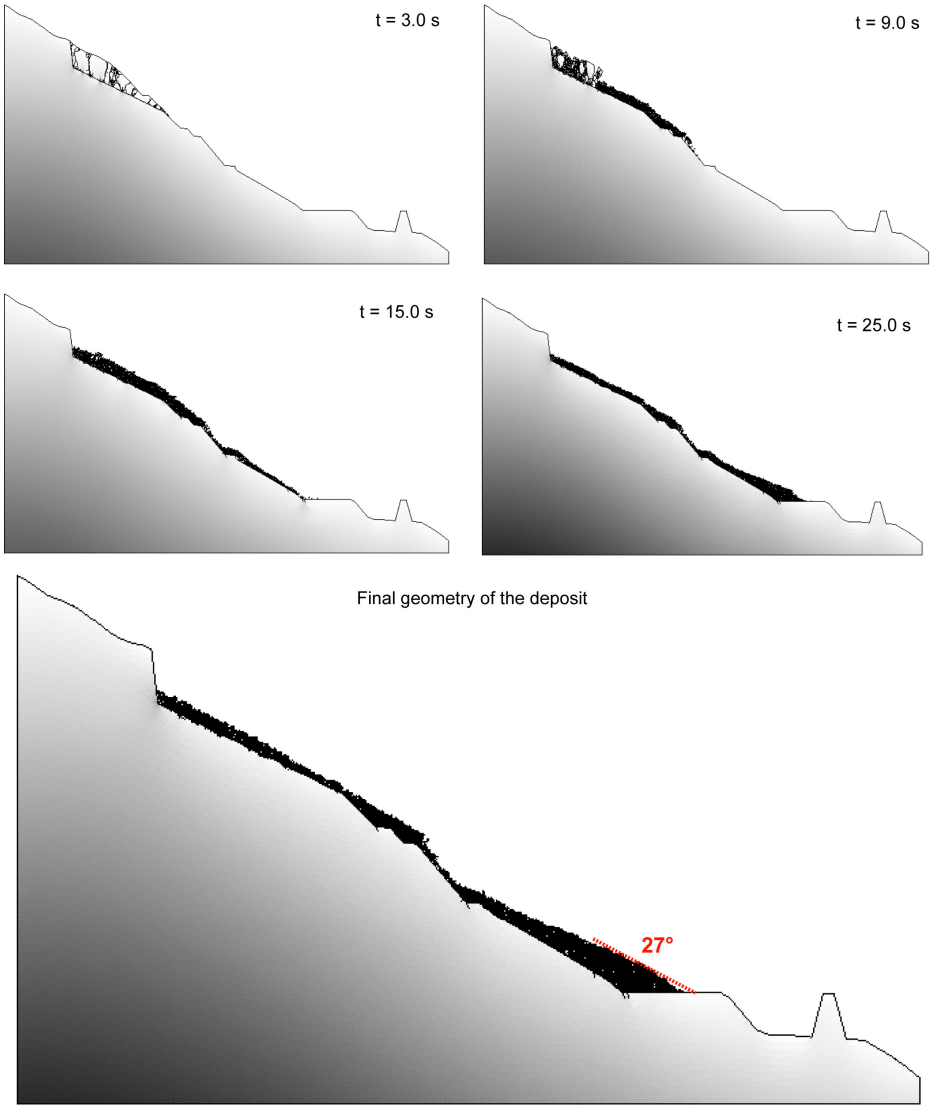

Figure 13 – Screenshots and final geometry of the main rock wedge runout FDEM simulation

Conclusions

The study described here shows the application of the FDEM and the Y-Geo software to the case study of the Torgiovannetto di Assisi rockslide. This involved geological and geomechanical characterization of the rock mass and the discontinuities as well as monitoring of the landslide behaviour by means of ground-based radar interferometry and a WSN consisting of wire and bar extensometers, tiltmeters, soil moisture probes, and a weather station. A back-analysis of the December 2005 collapse allowed the authors to validate the geotechnical model and define the characteristics of the numerical model to study the triggering conditions and the runout of the main rock wedge instability (182,000 m^3).

The following conclusions can be drawn from the work performed so far:

- The results of the numerical simulation of a uniaxial compression laboratory test performed on the Maiolica limestone are in good agreement with experimental data, confirming the capability of the FDEM to accurately model the fracture initiation and evolution as well as the brittle behaviour of intact rocks.

- FDEM and Y-Geo software, despite their limitations (mesh sensitivity, lack of hydro-mechanical coupling and fluid propagation in the cracks, long computational times), can effectively simulate complex slope instability problems from triggering, initiation, evolution, runout and deposition processes. An equivalent hydrostatic pressure was applied to simulate the progressive saturation of the main tension crack while, to simulate the increase of the pore pressure inside the marly-clayey material, the shear strength along the basal sliding plane was reduced. This represents a simplistic first step in including the influence of groundwater with the FDEM and Y-Geo. Eventually, the use of FDEM appeared to be a valid option when the landslides' evolution is mainly controlled by rock-fracturing processes. This is in agreement with previous research already mentioned. Although the results discussed will need more investigation, the example provided in this paper represents a further and more comprehensive step for the complete validation of this promising and relatively new numerical method thanks to the completeness of the data available, from geological and geotechnical characterization to monitoring data.

- The possibility of simulating the instability phenomena from the initiation to the end, makes the FDEM a useful numerical tool to carry out landslide scenario analyses, the results of which can be successively used for landslide risk assessment and management. Other methods (such as limit equilibrium or continuum and discontinuum numerical methods) could have been effectively adopted to study specific aspects of the slope instability problem (e.g., triggering conditions). In some cases, these may have been simpler to apply and certainly more validated, with respect to the FDEM. However, the possibility of using a single modeling tool to assess and predict the complete evolution of a landslide represents an advantage compared to the other methods.

- Despite the simplifications introduced in the simulation of the progressive saturation of joints and of the sliding surface, the velocities computed by the different FDEM simulations appear to be reasonable and realistic if compared to monitoring data. They could be effectively used to assist engineers and geoscientist to define thresholds for landslides early warning systems.

- Regarding the specific case of the Torgiovannetto rockslide, the results of the FDEM simulations indicate that the rock fall barrier and the quarry yard appear to be adequate to limit the downslope propagation of the collapsed material even in the worst-case scenario (i.e., the collapse of the whole 182,000-m^3 rock wedge).

Acknowledgements

The work described in this paper was funded by the Italian Ministry of Instruction, University and Research (MIUR) in the framework of the National Research Project PRIN 2009 titled "Integration of monitoring and numerical modeling techniques for early warning of large rockslides". The project was carried out by the Department of Earth Sciences of the Università degli Studi di Firenze (National coordinator and responsible for the Research Unit: Prof. Nicola Casagli), the Department of Electrical and Information Engineering "Guglielmo Marconi" of the Università degli Studi di Bologna (responsible for the Research Unit: Dr. Andrea Giorgetti) and the Department of Structural, Building and Geotechnical Engineering of Politecnico di Torino (responsible for the Research Unit: Dr. Marco Barla).

References

Alehossein, H., Hood, M., 1996. State of the art review of rock models for disc roller cutters. In: Aubertin, Hassani, Mitri (eds.), Rock Mechanics, Balkema, Rotterdam, 693–700.

An, B., Tannant, D.D., 2007. Discrete element method contact model for dynamic simulation of inelastic rock impact. Comp. & Geosci., 33, 513-521.

Antolini, F., 2014. The use of radar interferometry and finite-discrete modelling for the analysis of rock landslides. PhD Thesis, Politecnico di Torino, 273 pp.

Atzeni C., Barla M., Pieraccini M., Antolini F. 2015. Early warning monitoring of natural and engineered slopes with Ground-Based Synthetic Aperture Radar. In: Rock Mechanics and Rock Engineering, vol. 48 n. 1, pp. 235-246. - ISSN 0723-2632.

Balducci, M., Regni, R., Buttiglia, S., Piccioni, R., Venanti, L.D., Casagli, N., Gigli, G., 2011. Design and built of a ground reinforced embankment for the protection of a provincial road (Assisi, Italy) against rockslide. Proc. XXIV Conv. Naz. Geotecnica, AGI, Napoli, 22th-24th June 2011.

Barenblatt, I., 1962. Mathematical theory of equilibrium cracks in brittle fracture. Adv. Appl. Mech., 7, 55–129.

Barla, G., Antolini, F., Barla, M., Perino, A., 2013. Key aspects in 2D and 3D modeling for stability assessment of a high rock slope. In: Workshops 'Failure Prediction' 2013, Austrian Society for Geomechanics, Salzburg, 9th October 2013.

Barla, M., Antolini, F. 2015. An integrated methodology for landslides' early warning systems. Landslides, doi: 10.1007/s10346-015-0563-8.

Barla, M., Antolini, F., 2012. Integrazione tra monitoraggio e modellazione delle grandi frane in roccia nell'ottica dell'allertamento rapido. In: Barla G, Barla M, Ferrero A, Rotonda T (eds.), Nuovi metodi di indagine e modellazione degli ammassi rocciosi, MIR 2010, Torino 30th November – 1st December 2010, Pàtron, Bologna, 211–229. In Italian.

Barla, M., Piovano, G., Grasselli, G., 2011. Rock slide simulation with the combined finite discrete element method. Int. J. Geomech., 12, 711-721.

Brocca, L., Ponziani, F., Moramarco T., Melone F., Berni, N., Wagner, W., 2012. Improving Landslide Forecasting Using ASCAT-Derived Soil Moisture Data: A Case Study of the Torgiovannetto Landslide in Central Italy. Rem. Sens, 2012, 4 , 1232-1244.

Buratti, C., Giorgetti, A., Verdone, R., 2005. Cross layer design of an energy efficient cluster formation algorithm with carrier sensing multiple access for wireless sensor networks, EURASIP J. on Wireless Commun. and Networking, vol. 5, no. 5, pp. 672–685.

Canuti, P., Casagli, N., Gigli, G., 2006. Il modello geologico nelle interazioni fra movimenti di massa, infrastrutture e centri abitati. In: Barla, G., Barla, M. (eds.), Instabilità di versante, interazioni con le infrastrutture i centri abitati e l'ambiente, MIR 2006, Torino, 28th-29th November 2006, Pàtron, Bologna, 41–61. In Italian.

Cundall, P.A. & Strack, O.D.L., 1979 A discrete numerical model for granular assemblies. Géotech., 29(1), 47 –65.

Dowding, C. H., Belytschko, T. B., Yen, H. J., 1983. A coupled finite element–rigid block method for transient analysis of rock caverns. Int. J. Num. Anal. Meth. Geomech., 7(1), 117–127.

Dugdale, D.S., 1960. Yielding of steel sheets containing slits. J. Mech. Phys. Sol., 8, 100–104.

Evans, R., Marathe, M., 1968. Microcracking and stress-strain curves for concrete in tension. Mater. Struct., 1, 61–64.

FRANC2D/L [Computer Software]. Erin Iesulauro, Cornell Univ., Ithaca, NY.

Gigli, G., Casagli, N., Lombardi, L., Nocentini, M., 2007. Magnitude estimation and runout analyses of a rockslide in the Torgiovannetto quarry (PG). EGU 2007 – Geoph. Res. Abs., 9, 08399, 2007.

Giorgetti, A., Lucchi, M., Chiani, M., Win, M. Z., 2011. Throughput per Pass for Data Aggregation from a Wireless Sensor Network via a UAV, IEEE Trans. on Aerospace and Electronic Systems, vol. 47, no. 4, pp. 2610-2626.

Graziani, A., Rotonda, T., Tommasi, P., 2010. Fenomeni di scivolamento planare in ammassi stratificati: situazioni tipiche e motodi di analisi. In: G. Barla, M. Barla (Eds.), Problemi di stabilità nelle opere geotecniche, MIR 2010, Torino, November 30th- Dicember 1st 2010, Pàtron, Bologna. 93-124

Graziani, A., Marsella, M., Rotonda, T., Tommasi, P., Soccodato, C., 2009. Study of a rock slide in a limestone formation with clay interbeds. Proceedings of International Conference on Rock Joints and Jointed Rock Masses, Tucson, Arizona, USA 7th-8th January 2009.

Hart, J.K., Martinez, K. 2006. Environmental sensor networks: A revolution in the earth system science? Earth-Science Reviews, vol. 78, no. 3, pp. 177–191.

Ida, Y., 1972. Cohesive force across the tip of a longitudinal-shear crack and Griffith's specific surface energy. J. Geoph. Res., 77, 3796–3805.

Intrieri, E., Gigli, G., Mugnai F., Fanti, R., Casagli, N., 2012. Design and implementation of a landslide early warning system. Eng. Geol., 147-148 (2012), 124-136.

Lisjak, A., Grasselli G., 2010. Rock impact modelling using FEM/DEM. Proceedings of 5th International Conference on Discrete Elements Methods – DEM5, 25th-26th August, 2010, London, United Kingdom, 6 pp.

Lisjak, A., Grasselli G., 2011. Combined finite-discrete element analysis of rock slope stability under dynamic loading. Proceedings of 2011 PAN-American CGS Geotechnical Conference, 2nd-6th October 2011, Toronto, Canada, 8 pp.

Lisjak, A., Liu, Q., Zhao, Q., Mahabadi, O.K., and Grasselli, G., 2013. Numerical simulation of acoustic emission in brittle rocks by two-dimensional finite-discrete element analysis. Geoph. J. Int., doi:10.1093/gji/ggt221.

Lorig, L.J., Brady, B.H., Cundall P.A., 1986. Hybrid distinct element-boundary element analysis of jointed rock. Int. J. Rock. Mech. Min. Sci. Geomech. Abstr., 23 (4), 303–312.

Mahabadi, O.K., Grasselli, G., Munjiza, A., 2010a. Y-GUI: A graphical user interface and pre-processor for the combined finite-discrete element code, Y2D, incorporating material inhomogeneity. Comp. Geosci., 36, 241–252.

Mahabadi, O. K., Lisjak, A., Grasselli, G., Lukas, T., Munjiza, A., 2010b. Numerical modelling of a triaxial test of homogeneous rocks using the combined finite-discrete element method. In: Zhao, J., Labiouse, V., Dudt, J.,. Mathier, J. (eds). Proc. of Rock Mechanics in Civil and Environmental Engineering (Eurock 2010), A.A. Balkema, Lausanne, Switzerland, 173–176.

Mahabadi, O.K., Lisjak, A., Munjiza, A., Grasselli, G., 2012. Y-Geo: New Combined Finite-Discrete Element Numerical Code for Geomechanical Applications. Int. J. Geomech., 12, Special Issue: Advances in Modeling Rock Engineering Problems, 676–688.

Malvar, L.J., & Warren, G.E., 1988. Fracture energy for three-point bending test on single-edge notched beams. Exp. Mech., 28(3), 226-272.

Munjiza, A., 2004. The combined Finite-Discrete Element Method. John Wiley & Sons, New York, 333 pp.

Munjiza, A., Andrews K., 2000. Penalty function method for combined finite-discrete element systems comprising large number of separate bodies. Int. J. Num. Meth. Eng., 49(11), 1377-1396.

Munjiza, A., John, N.W.M., 2002. Mesh size sensitivity of the combined FEM/DEM fracture and fragmentation algorithms. Eng. Fract. Mech., 69(2002), 281-295.

Munjiza, A., Owen, D., Bicanic, N., 1995. A combined finite-discrete element method in transient dynamics of fracturing solids. Eng. Computation, 12(2), 145-174.

Mustoe, G.G.W., 1992. A generalized formulation of the discrete element method. Eng. Computation, 9(2), 181 – 190.

Piovano, G., Antolini, F., Barla, M., Barla G. 2013. Continuum-discontinuum modelling of failure and evolution mechanisms of deep seated landslides. In: 6th International Conference on Discrete Element Method, Golden, USA, 5-6 August 2013, 295-300.

Piovano, G., Barla, G., Barla, M., 2011. FEM/DEM modeling of a slope instability on a circular sliding surface. Proc. of IACMAG 2011, Melbourne, Australia, 9-11 May 2011, 6 pp.

ELFEN 2.8 [Computer Software]. Rockfield Software Ltd., Swansea (UK).

Salciarini, D., Tamagnini, C., Conversini P., 2009. Discrete element modeling of debris-avalanche impact on earthfill barriers. Phys. Chem. Earth, 35 (2010), 172–181.

CUBIT 11.1 [Computer Software]. Sandia National Laboratories, Albuquerque, New Mexico (USA).

Saouma, V.E., Kleinosky, M-J., 1984. Finite element simulation of a rock cutting: a fracture mechanics approach. Proceedings of ASCE 1984 - 25th U.S. Symposium on Rock Mechanics (USRMS), 25-27 June, Evanston, Illinois, 792–799.

Stead, D., Coggan J., 2006. Numerical modelling of rock slopes using a total slope failure approach. In: Evans S.G., Scarascia Mugnozza G., Strom A., Hermanss R.L. (eds.) - Landslides from massive rock slope failure. Proceedings of the NATO Advanced Reasearch Workshop on Massive Rock Slope failure: New Models for Hazard Assessment, Celano, Italy, 16th-21th June 2002, Springer, The Netherlands, 129-138.

Stead, D., Coggan, J., Eberhardt, E., 2004. Realistic simulation of rock slope failure mechanisms: the need to incorporate principles of fracture mechanics. Regional ISRM Sinorock 2004 Symposium, Int. J. Rock Mech. Min. Sci., 41, 1-6.

Stead, D., Eberhardt, E., Coggan, J., 2006. Developments in the characterization of complex rock slope deformation and failure using numerical modelling techniques. Eng. Geol., 83, 217-235.

Swenson, D.V., Ingraffea A.R., 1988. Modelling mixed-mode dynamic crack propagation using finite elements: theory and applications. Comp. Mech., 3, 187-192.

Verdone, R., Dardari, D., Mazzini, G., Conti, A., 2010. Wireless Sensor and Actuator Networks. Elsevier Science.

Wawrzynek. P., Ingraffea, A.R., 1989. An interactive approach to local remeshing around a propagation crack. Finite Elements in analysis and design, 5, 87-96.

Williams, J., Hocking, G., Mustoe, G:G:W., 1985. The theoretical basis of discrete element methods. In: Middleton, J. and Pande, G.N. (eds.) "NUMETA 85, Proceedings of the International Congress on Numerical Methods in Engineering, Swansea", 897-906.